Fluoroquinolones: novel class of gastrointestinal dietary lipid digestion and absorption inhibitors

Yusuf M. Al-Hiari, Violet N. Kasabri, Ashok K. Shakya, Muhammad H. Alzweiri, Fatma U. Afifi, Yasser K. Bustanji & Ihab M. Al-Masri

Springer

Springer

**MEDICINAL
CHEMISTRY
RESEARCH**

ORIGINAL RESEARCH

Fluoroquinolones: novel class of gastrointestinal dietary lipid digestion and absorption inhibitors

**Yusuf M. Al-Hiari · Violet N. Kasabri · Ashok K. Shakya ·
Muhammad H. Alzweiri · Fatma U. Afifi ·
Yasser K. Bustanji · Ihab M. Al-Masri**

Abstract Pancreatic triacylglycerol lipase (PL) has been reported as an interesting pharmacological target for the management of dyslipidemia, atherosclerosis, and obesity. In the current study, a 4-quinoline-3-carboxylic acid system has been identified as a potent inhibitor of PL. Three new fluoroquinolones (**11**, **12,** and **13**) were synthesized and evaluated in vitro with respect to their anti-lipase efficacy and potency properties and gave IC_{50} values in the range of 18.4–29.1 μM against PL. The IC_{50} of the standard drug orlistat was 0.2 μM. The inhibitory activities of these compounds were supported by docking studies, which suggested that they acted according to a similar mechanism to that of the known drug orlistat. In conclusion, these effective PL inhibitors could be used to advance the development of anti-obesity drugs via the regulation of the entire gastrointestinal lipolysis process.

Y. M. Al-Hiari (✉) · V. N. Kasabri · M. H. Alzweiri ·
F. U. Afifi · Y. K. Bustanji
Faculty of Pharmacy, The University of Jordan, Amman 11942,
Jordan
e-mail: hiary@ju.edu.jo

A. K. Shakya
Faculty of Pharmacy and Medical Sciences, Al-Ahliyya Amman
University, Amman 19328, Jordan

I. M. Al-Masri
Faculty of Pharmacy, Al-Azhar University, Gaza, Gaza strip,
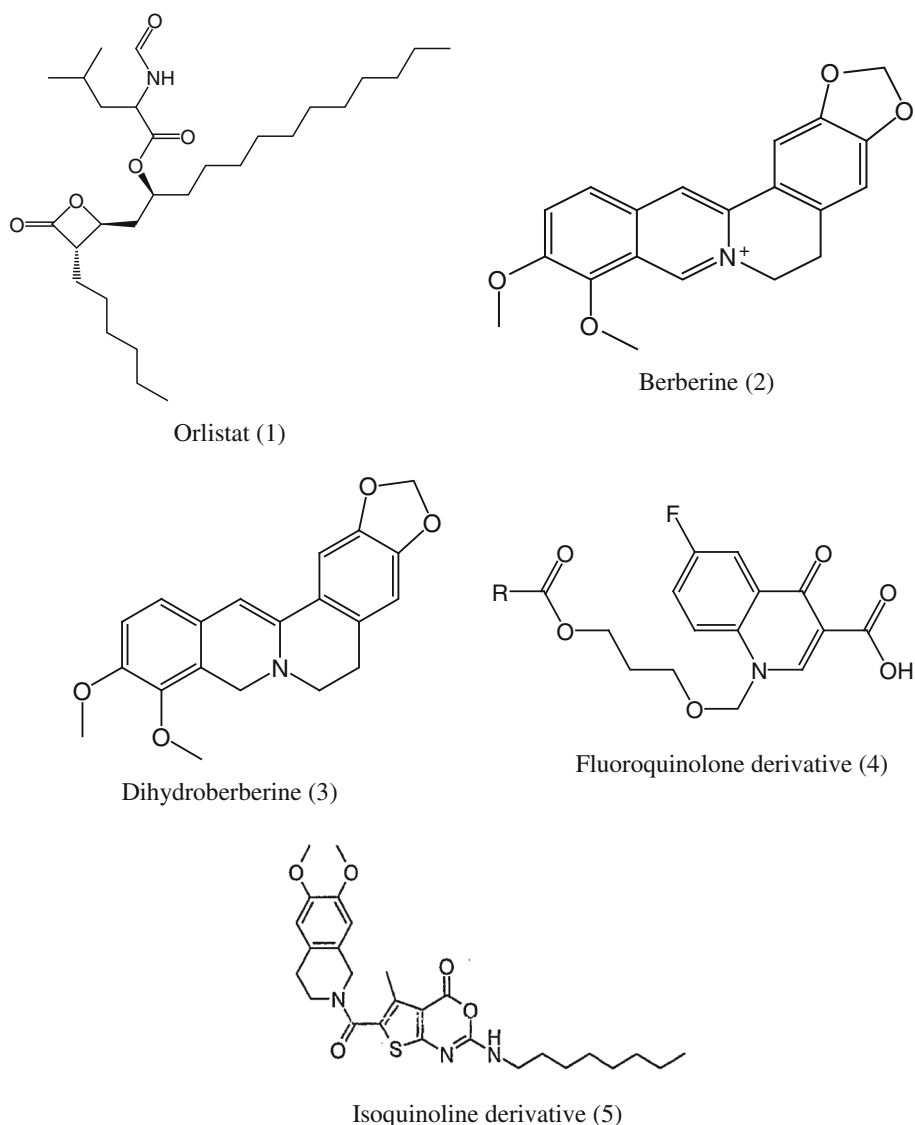Palestine

Introduction

The level of interest in the development of potential anti-obesity agents has increased significantly in recent years, because obesity is reaching epidemic proportions throughout the world (Baretic, 2012; WHO, 2012). Orlistat (**1**, Fig. 1) is the only FDA-approved pancreatic lipase (PL) inhibitor currently available in the United States and Europe (Baretic, 2012). While many anti-obesity drugs had previously been released as commercial products, they were subsequently removed from the market because they produced a variety of unwanted side effects. Several studies have been conducted to explore the use of multiple agents for the safe and effective management of dyslipidemia and/or obesity via the inhibition of lipid-metabolizing enzymes, because the inhibition of these enzymes can lead to a reduction in the digestion and absorption of dietary lipids (Ninomiya *et al.*, 2004; Yamada *et al.*, 2008; Clifton *et al.*, 2010; Chen *et al.*, 2012). Ebdrup *et al.* (2004) reported the synthesis and structure–activity relationships of a novel class of potent and selective carbamoyl-based inhibitors of hormone-sensitive lipase. In addition, natural products, such as berberine (**2**) and dihydroberberine (**3**, Fig. 1), which are isoquinoline derivatives, have been reported as PL inhibitors (Mohammad *et al.*, 2013). A variety of different synthetic heterocyclic compounds have also been prepared and evaluated as PL inhibitors, including fluoroquinolone (FQ, **4**) (De la Cruz *et al.*, 1991) and isoquinoline (**5**, Fig. 1), but these compounds showed very low levels of activity (Witter and Castelhano, 2006). In contrast, several quinoline derivatives have been reported as ileal bile acid transporter inhibitors (IBAT inhibitors) (Charmot, 2012). IBAT inhibitors selectively inhibit the reuptake of bile acids in the ileum, leading to an increase in fecal elimination as well as triggering the biosynthesis of biliary salts from the cholesterol pool.

Fig. 1 Structure of different heterocycle compounds cited as pancreatic triacylglycerol lipase inhibitor

Orlistat (1)

Berberine (2)

Dihydroberberine (3)

Fluoroquinolone derivative (4)

Isoquinoline derivative (5)

As part of a recent screening project aimed at identifying potential PL inhibitors (Bustanji *et al.*, 2011) as anti-obesity agents, berberine (**2**) and dihydroberberine (**3**) were shown to exhibit inhibitory activity toward PL (Bustanji *et al.*, 2011; Mohammad *et al.*, 2013). Similarities between the basic scaffold of the isoquinoline alkaloids (**2**, **3**) and the quinolone motif prompted us to evaluate the potential anti-lipase activity of a series of novel synthetic FQ derivatives. Molecular modeling studies involving FRED were used to validate the experimental data.

Materials and methods

Chemistry

All of the chemicals and solvents used in the current study were purchased as the analytical grade and used directly

without further purification. 2,4-Dichloro-5-fluoro-3-nitrobenzoic acid, ethyl 3-(*N*,*N*-dimethyl-amino) acrylate, ethyl amine, and 2-aminobenzoic acid were purchased from Acros (Geel, Belgium). Sodium bicarbonate, sodium dithionite, and polyphosphoric acid (PPA) were purchased from Sigma-Aldrich (St. Luis, MO, USA). Nuclear magnetic resonance spectra (NMR) were recorded on a Varian Oxford-300 (300 MHz) spectrometer (Varian Inc., Palo Alto, California, USA) and Bruker Advance DPX-300 (300 MHz) spectrometer (Bruker, Bellirica, Massachusetts, USA). The chemical shifts were reported in ppm relative to tetramethylsilane (TMS), which was used as an internal reference standard. Deuterated dimethylsulfoxide (DMSO-d_6) and chloroform (CDCl$_3$) were used as the NMR solvents. ^{1}H NMR data were reported in the following way: chemical shift (ppm), multiplicity, coupling constant (Hz), number of protons, and the corresponding proton(s). Infrared (IR) spectra were recorded using Shimadzu 8400F

FT-IR spectrophotometer (Shimadzu, Kyoto, Japan). The samples were prepared as potassium bromide (KBr) (Merck, Darmstadt, Germany) disks. Colorimetric data were recorded using double beam UV–Vis spectrophotometer SpectroScan 80D (Sedico Ltd, Nicosia, Cyprus). Melting points (mp) were determined in open capillaries on a Stuart scientific electro-thermal melting point apparatus (Stuart, Staffordshire, UK) and are uncorrected. High-resolution mass spectra (HRMS) were measured in the positive or negative ion mode using an electrospray ionizer (ESI) and an ion trap analyzer on a Bruker APEX-4 (7 Tesla) instrument (Bruker, Bellirica, Massachusetts, USA). The samples were dissolved in acetonitrile, diluted in spray solution (methanol/water 1:1—v/v containing 0.1 % formic acid) and infused using a syringe pump with a flow rate of 120 μl/min. An external calibration was conducted using an arginine cluster in a mass range (m/z) of 175–871. Thin layer chromatography (TLC) was performed on aluminum plates pre-coated with fluorescent silica gel GF_{254} from ALBET (Filalbet, S. L., EEC). Silica Gel (70–230 Mesh) from GCC (Sandycroft, Clwyd, UK) was used for preparative TLC, and the plates were visualized by UV using a Spectroline CX-20 cabinet (Spectronic Corp., Westbury, NY, USA). The mobile phases were made up as follows: System (1): chloroform ($CHCl_3$): methanol (MeOH): formic acid (FA) (94:5:1); System (2): $CHCl_3$:MeOH:FA (90:10:1); System (3): hexane:ethyl acetate (50:50); System (4): System (1): system (3) (50:50).

(Z/E) Ethyl-3-(N,N-dimethylamino)-2-(2,4-dichloro-5-fluoro-3-nitrobenzoyl) acrylate (7)

Under strictly anhydrous conditions, a mixture of the benzoic acid derivative 6 (10.2 g, 40 mmol) and thionyl chloride (19.0 g, 160 mmol) in dry benzene (120 mL) was heated at 75–80 °C for 3–4 h. The mixture was then distilled to dryness under reduced pressure to give the crude product as a residue, which was evaporated from benzene (2 × 20 mL) to remove any residual thionyl chloride. The resulting 2,4-dichloro-5-fluoro-3-nitrobenzoyl chloride (6a) was used in the next step without further purification.

A solution of the crude acid chloride 6a in dry benzene (25 mL) was added in a drop-wise manner to a cooled solution of ethyl 3-(N,N-dimethyl-amino)acrylate (6.3 g, 44 mmol) and triethylamine (4 mL, 8.1 g, 80 mmol) in dry benzene (50 mL) at 5–10 °C under anhydrous conditions. The resulting mixture was stirred continuously for 2 h at room temperature before being heated at reflux for 1.5 h. The mixture was then cooled to ambient temperature and distilled to dryness under reduced pressure to give the crude product, which was dissolved in $CDCl_3$. The resulting solution was washed with water (30 mL), dried over anhydrous $MgSO_4$, and concentrated under reduced

pressure to give a residue (about 20 mL), which was soaked in methanol (10 mL) to give 7 as a yellowish precipitate, which was collected by filtration and dried under vacuum at 40 °C, mp = 139–141 °C (decomposition), yield $\approx$ 13.8 g (91 %), R_f value in system (1) = 0.89 and in system (2) = 0.90. IR (KBr): v 3,431, 3,073, 2,987, 2,928, 2,864, 1,689, 1,619, 1,553, 1,455, 1,421, 1,374, 1,344, 1,321, 1,278, 1,205, 1,177, 1,129, 1,030 cm^{-1}. ^{1}H NMR (300 MHz, $CDCl_3$): δ 0.95 (t, $J = 7.1$ Hz, 3H, OCH_2CH_3), 2.97, 3.37 (2 s, each 3H, $N (CH_3)_2$), 3.94 (q, $J = 7.1$ Hz, 2H, OCH_2Me), 7.27 (d, $^3J_{H-F} = 8.2$ Hz, 1H, H-6′), 7.91 (br s, 1H, N–C(3)–H). ^{13}C NMR (75 MHz, $CDCl_3$): δ 13.8 (CH_3CH_2), 43.3, 48.4 [$N (CH_3)_2$], 60.2 (CH_2Me), 100.9 (C-2), 114.5 (d, $^2J_{C-F} = 23.3$ Hz, C-4′), 116.9 (d, $^2J_{C-F} = 23.1$ Hz, C-6′), 118.2 (d, $^3J_{C-F} = 4.5$ Hz, C-1′), 144.2 (d, $^3J_{C-F} = 6$ Hz, C-3′), 148.8 (br d, $^4J_{C-F} = 1.3$ Hz, C-2′), 156.6 (d, $^1J_{C-F} = 254$ Hz, C-5′), 160.5 (N–C-3), 166.5 (CO_2Et), 185.1 (C=O). HRMS (ESI, +ve): m/z calculated for $C_{14}H_{14}Cl_2FN_2O_5$ $[M+H]^+$: 379.02638, Found: 379.02591. Anal. calcd. for $C_{14}H_{13}Cl_2FN_2O_5$ (379.17): C, 44.35; H, 3.46; N, 7.39. Found: C, 44.30; H, 3.38; N, 7.62.

(Z/E) Ethyl 2-(2,4-dichloro-5-fluoro-3-nitrobenzoyl)-3-ethylamino-acrylate (8)

A mixture of ethyl-3-(N,N-dimethylamine)-2-(2,4-dichloro-5-fluoro-3-nitrobenzoyl) acrylate (7, 13.5 g, 36 mmol) and ethyl amine (6.4 g, 72 mmol) in methanol (20 mL) was stirred at −6 °C for 30 min. After 1 h, the precipitate thus formed was filtered and washed with diethyl ether (3 mL) to give the desired product 8 as a white solid, which was used without further purification in the next step, mp = 140–142 °C (decomposition), yield $\approx$ 13.2 g (97 %), R_f value in system (1) = 0.93. IR (KBr): v 3,435, 3,198, 3,075, 3,040, 2,987, 2,911, 1,681, 1,615, 1,552, 1,431, 1,366, 1,265, 1,199, 1,155, 1,072, 1,028 cm^{-1}. ^{1}H NMR (300 MHz, $CDCl_3$): δ 0.93, 1.06(Z/E, 2t, $J = 7.16, 7.17$ Hz, 3H, NH–CH_2CH_3), 1.41, 1.62 (Z/E, 2t, $J = 7.3, 7.29$ Hz, 3H, OCH_2CH_3), 3.55, 3.56 (Z/E, 2q, $J = 6.5, 7.14$ Hz, 2H, NH–CH_2CH_3), 4.0, 4.04 (Z/E, 2q, $J = 7.13, 7.26$ Hz, 2H, OCH_2CH_3), 7.16, 7.21 (Z/E, 2d, $^3J_{H-F} = 8.1, 8.13$ Hz, 1H, H-6′), 8.23, 8.33 (Z/E, 2d, $J = 14.29, 14.79$ Hz, 1H, N–C(3)–H), 11.100, 11.12 (Z/E, 2 br d, $J = 16$ Hz, 1H, exchangeable N–H). ^{13}C NMR (75 MHz, $CDCl_3$): δ 13.32, 13.82 (Z/E, NCH_2CH_3), 15.64, 15.65 (Z/E, OCH_2CH_3), 45.23, 45.44 (Z/E, NCH_2CH_3), 59.96, 60.16 (Z/E, OCH_2CH_3), 99.58, 99.79 (Z/E, C-2), 114.15, 114.2 (Z/E, 2d, $^2J_{C-F} = 23.25$ Hz, C-4′), 115.75, 115.96 (Z/E, 2d, $^2J_{C-F} = 23.25, 22.88$ Hz, C-6′), 117.71, 117.89 (Z/E, 2d, $^3J_{C-F} = 5.8$ Hz, C-1′), 143.72, 143.95 (d, $^3J_{C-F} = 6.2$ Hz, C-3′), 154.95 (br d, $^4J_{C-F} = 1.0$ Hz, C-2′), 156.33 (d, $^1J_{C-F} = 255$ Hz, C-5′), 160.58, 161.20 (Z/E, N–C-3),

165.90, 167.72 (Z/E, CO_2Et), 188.27 (C=O). HRMS (ESI, +ve): calculated for $C_{14}H_{14}Cl_2FN_2O_5$ $[M+H]^+$: 379.02638, Found: 379.02583. Anal. calcd. for $C_{14}H_{13}Cl_2FN_2O_5$ (379.17): C, 44.35; H, 3.46, N, 7.39. Found: C, 44.38; H, 3.56; N, 7.82.

Ethyl 7-chloro-1-ethyl-6-fluoro-8-nitro-4-oxo-1, 4-dihydroquinoline-3-carboxylate (9)

A mixture of **8** (11.7 g, 30 mmol) and potassium carbonate (11.7 g, 85 mmol) in dimethyl-formamide (DMF, 50 mL) was heated at 85 °C with continuous stirring for 1 h. The reaction mixture was then poured onto crushed ice (500 g) with vigorous stirring to give a precipitate, which was collected by suction filtration and dried in the absence of light to give the desired compound **9** as a faint yellow solid, mp = 160–164 °C (decomposition), yield ≈ 10.4 g (87 %), R_f value in system (1) = 0.89. IR (KBr): v 3,095, 2,975, 2,905, 2,341, 1,735, 1,655, 1,612, 1,554, 1,474, 1,431, 1,385, 1,356, 1,265, 1,245, 1,174, 1,132, 1,048 cm^{-1}.^{1}H NMR (300 MHz, $CDCl_3$): δ 1.37–1.47 (2t, $J = 7.2$ Hz, 6.3 Hz, 6H, 2CH_3), 4.04 (q, $J = 7.2$ Hz, 2H, NCH_2Me), 4.38 (q, $J = 7.2$ Hz, 2H, OCH_2Me), 8.47 (d, $^3J_{H-F} = 8.4$ Hz, 1H, H-5), 8.45 (s, 1H, H-2). ^{13}C NMR (75 MHz, $CDCl_3$): δ 14.35 (NCH$_2$$CH_3$), 16.30 (OCH$_2$$CH_3$), 50.52 (N$CH_2CH_3$), 61.52 (O$CH_2CH_3$), 109.20 (C-3), 115.91 (d, $^2J_{C-F} = 22.73$ Hz, C-5), 122.32 (d, $^2J_{C-F} = 24.21$ Hz, C-7), 129.20 (C-4a), 133.53 (C-8a), 141.42 (C-8), 151.32 (C-2), 153.23 (d, $^1J_{C-F} = 255.0$ Hz, C-6), 164.29 (C(3)–CO_2Et), 171.10 (C-4). HRMS (ESI, +ve): calculated for $C_{14}H_{13}ClFN_2O_5$ $[M+H]^+$: 343.04970, Found (343.04915). Anal. calcd. for $C_{14}H_{12}ClFN_2O_5$ (342.71): C, 49.07; H, 3.53; N, 8.17. Found: C, 49.31; H, 3.35; N, 8.37.

7-Chloro-1-ethyl-6-fluoro-8-nitro-4-oxo-1,4-dihydroquinoline-3-carboxylic acid (10)

Compound **9** (10.4 g, 30.4 mmol) was dissolved in a 150-mL mixture of concentrated H_2SO_4, H_2O, and 96 % ethanol (1:1:1—v/v/v), and the resulting mixture was heated at 80–85 °C under reflux conditions for 48 h. The crude product was cooled and poured onto crushed ice (250 g) to give a precipitate, which was collected by filtration, washed with cold water (2 × 20 mL), dried, and recrystallized from a mixture of chloroform and methanol (50 mL; 1:1) to give the desired product **10** as a yellow solid, mp = 239–241 °C, yield ≈ 8.8 g (92 %), R_f value in system (1) = 0.70, R_f value in system (3) = 0.50. IR (KBr): v 3,065, 2,586, 1,725, 1,630, 1,580, 1,544, 1,452, 1,365, 1,332, 1,285, 1,255, 1,225, 1,132, 1,054 cm^{-1}. ^{1}H NMR (300 MHz, $CDCl_3$): δ 1.52 (t, $J = 7.2$ Hz, 3H, CH_2CH_3), 4.19 (q, $J = 7.2$ Hz, 2H, CH_2CH_3), 8.50 (d, $^3J_{C-F} = 7.8$ Hz, 1H, H-5), 8.79 (s, 1H, H-2), 13.78 (s, 1H, CO_2H).^{13}C NMR (75 MHz, DMSO-d_6): 16.28 (CH_3), 51.43 (CH_2), 110.26 (C-3), 115.08 (d,

$^2J_{C-F} = 22.82$ Hz, C-5), 122.82 (d, $^2J_{C-F} = 23.3$ Hz, C-7), 128.37 (C-4a), 132.53 (C-8a), 146.94 (C-8), 151.41 (C-2),154.98 (d, $^1J_{C-F} = 253.73$ Hz, C-6), 164.92 (C(3)–CO_2H), 175.69 (C-4). HRMS (ESI, +ve): calculated for $C_{12}H_9ClFN_2O_5$ $[M+H]^+$: 315.01840, Found: 315.01792. Anal. calcd. for $C_{12}H_8ClFN_2O_5$ (314.65): C, 45.81; H, 2.56; N, 8.90. Found: C, 46.01; H, 2.46; N, 8.95.

7-[(2-Carboxyphenyl)amino]-1-ethyl-6-fluoro-8-nitro-4-oxo-1,4-dihydroquinoline-3-carboxylic acid (11)

A mixture of 2-aminobenzoic acid (1.25 g, 9 mmol), **10** (1.0 g, 3 mmol), and sodium hydrogen carbonate (1.5 g, 18 mmol) in 70 % aqueous ethanol (140 mL) was refluxed at 70–75 °C for 6–7 days. The resulting mixture was cooled to ambient temperature and washed with dichloromethane (2 × 50 mL). The organic layers were discarded and the aqueous layer was cooled to room temperature before its pH was adjusted to 6–7 by the addition of 3.5 N HCl. The mixture was then washed with CH_2Cl_2 (50 mL) and acidified further to a pH in the range of 1–2 to give the title compound as yellow/brown precipitate, which was collected by filtration, washed with cold water (2 × 10 mL), dried, and recrystallized from a mixture of chloroform and ethanol (1:1—v/v) to give the desired compound **11** as a yellow/brown solid, mp = 252–254 °C (decomposition), yield ≈ 1.1 g (88 %), R_f value in system (1) = 0.70, R_f value in system (3) = 0.78. IR: v 3,055, 2,874, 2,360, 2,342, 1,748, 1,670, 1,616, 1,543, 1,451, 1,254, 1,095, 806,764 cm^{-1}.^{1}H NMR (300 MHz, DMSO-d_6) : δ1.35 (t, $J = 6.90$ Hz, 3H, CH_3), 4.23 (q, $J = 6.60$ Hz, 2H, CH_2), 6.87 (dd, $J = 7.20$ Hz, 6.60 Hz, 1H, H-6''), 7.04 (dd, $J = 7.50$ Hz, 7.50 Hz, 1H, H-4''), 7.47 (dd, $J = 7.80$, 7.50 Hz, 1H, H-5''), 7.95 (d, $J = 7.80$ Hz, 1H, H-3''), 8.38 (d, $^3J_{H-F} = 11.10$ Hz, 1H, H-5), 9.02 (s, 1H, H-2), 10.32 (br s, 1H, NH–Ar), 13.65 (br s, 1H, Ar–CO_2H), 14.25 (br s, 1H, C(3)–CO_2H, overlapping with Ar–CO_2H).^{13}C NMR (75 MHz, DMSO-$d6$): 15.97 (CH_3), 51.48 (CH_2), 109.79 (C-3), 115.21 (C-4a), 115.71 (d, $^2J_{C-F} = 21.3$ Hz, C-5), 116.71 (d, C-6''), 121.51 (C-4''), 124.60 (d, $^3J_{C-F} = 7.43$ Hz, C-8), 129.85 (d, $^2J_{C-F} = 17.18$ Hz, C-7), 130.62 (C-8a), 131.60 (C-5''), 134.53 (C-3''), 137.92 (C-2''), 144.34 (C-1''), 152.31 (C-2), 153.69 (d, $^1J_{C-F} = 253.73$ Hz, C-6), 165.25 (C(3)–CO_2H), 170.20 (Ar–$COOH$), 175.73 (C-4). HRMS (ESI, −ve): m/z calculated for $C_{19}H_{13}FN_3O_7$ $[M−H]^-$: 414.07376, Found 414.07370. Anal. calcd. for $C_{19}H_{14}FN_3O_7$ (415.33): C, 54.95; H, 3.40; N, 10.12. Found: C, 54.55; H, 3.31; N, 9.92.

8-Amino-7-[(2-carboxyphenyl)amino]-1-ethyl-6-fluoro-4-oxo-1,4-dihydroquinoline-3-carboxylic acid (12)

A solution of sodium dithionite (0.87 g, 5 mmol) in water (5 mL) was added dropwise to a stirred suspension of

compound **11** (0.43 g, 1 mmol) and potassium carbonate (0.96 g, 7 mmol) in water (20 mL), and the resulting mixture was stirred for 30 min at ambient temperature. The pH of the solution was adjusted to about 4, and the resulting precipitate was collected by filtration, washed with water, air-dried, and recrystallized from acetone and ethanol (1:1—v/v) to give the title compound **12** as faint yellow crystals, mp = 238–240 °C (decomposition), yield ≈ 0.38 g (98 %), R_f value in system (1) = 0.58, R_f value in system (2) = 0.55. IR: v 3,422, 3,337, 3,055, 1,717, 1,609, 1,543, 1,501, 1,454, 1,389, 1,339, 1,250, 1,161, 1,084, 806, 752 cm^{-1}. ^{1}H NMR (300 MHz, DMSO-d_6): 1.23 (t, $J = 6.60$ Hz, 3H, CH_3), 4.84 (q, $J = 6.90$ Hz, 2H, CH_2), 5.74 (br s, 2H, NH_2), 6.35 (d, $J = 8.40$ Hz, 1H, H-6″), 6.81 (dd, $J = 7.50$ Hz, 7.5 Hz, 1H, H-4″), 7.34 (dd, $J = 7.50$ Hz, 7.50 Hz, 1H, H-3″), 7.50 (d, $^3J_{H–F} = 9.60$ Hz, 1H, H-5), 7.94 (d, $J = 7.50$ Hz, 1H, H-5″), 8.95 (s, 1H, H-2), 9.35 (br s, 1H, NH–Ar), 14.0–15.20 (2 br s, 2H, C(3)–CO$_2$H and Ar–CO$_2$H overlapping). ^{13}C NMR (75 MHz, DMSO-d_6): 16.21 (CH_3), 52.52 (CH_2), 99.53 (d, $^2J_{C–F} = 23.6$ Hz, C-5), 107.62 (C-3), 113.54 (d, $J = 5.28$ Hz, C-6″), 118.13 (C-4″), 120.36 (d, $^2J_{C–F} = 17.30$ Hz, C-7), 122.21 (C-8), 127.16 (d, $^3J_{C–F} = 7.43$ Hz, C-4a), 129.92 (C-8a), 132.01 (C-3″), 134.62 (C-5″), 140.64 (d, $J = 3.38$ Hz, C-2″), 148.01 (C-1″), 151.54 (C-2), 157.28 (d, $^1J_{C–F} = 244$ Hz, C-6), 166.41 (C(3)–CO$_2$H), 170.49 (C(2″)–CO$_2$H), 177.39 (C-4). HRMS (ESI, −ve): m/z calculated for C$_{19}$H$_{15}$FN$_3$O$_5$ [M−H]$^-$: 384.09958, Found 384.09662. Anal. calcd. for C$_{19}$H$_{16}$FN$_3$O$_5$ (385.11): C, 59.22; H, 4.19; N, 10.90. Found: C, 59.34; H, 4.13; N, 10.54.

1-Ethyl-6-fluoro-4, 12-dioxo-4, 7, 12, 13-tetrahydro-1H-quino [7,8-b] [1,4]benzodiazepine-3-carboxylic acid (13)

A stirred solution of compound **12** (0.2 g, 0.5 mmol) and PPA (10 mL) was refluxed for 3 h at 150–160 °C. The resulting mixture was cooled to 50 °C and poured onto cold water (60 mL) with vigorous stirring to give a precipitate, which was collected by suction filtration, washed with water (2 × 10 mL), and dried to give the desired compound **13** as a yellow/green solid, mp = 314–317 °C (decomposition), yield ≈ 0.18 g (98 %), R_f value system (1) = 0.60, R_f value in system (2) = 0.65; R_f value system (3) = 0.32. IR: v 3,291, 3,233, 3,051, 2,982, 2,342, 1,705, 1,667, 1,620, 1,593, 1,474, 1,443, 1,424, 1,369, 1,342, 1,234, 806, 772 cm^{-1}. ^{1}H NMR (300 MHz, DMSO-d_6): 1.08 (t, $J = 6.60$ Hz, 3H, CH_3), 4.70 (q, $J = 6.80$ Hz, CH_2), 7.11 (dd, $J = 7.50$, 7.50 Hz, 1H, H-10), 7.28 (d, $J = 8.10$ Hz, 1H, H-8), 7.47 (dd, $J = 7.50$, 7.80 Hz, 1H, H-9), 7.75 (dd, $J = 7.8$, 3.0 Hz, 1H, H-11), 7.89 (d, $^3J_{H–F} = 10.0$ Hz, 1H, H-5), 8.69 (d, $J = 2.50$ Hz, 1H, N(7)–H), 8.94 (s, 1H, H-2), 10.13 (br s, 1H, N(13)–H), 15.51 (br s, 1H, COOH). ^{13}C NMR (75 MHz, DMSO-d_6): 13.88

(CH_3), 53.33 (CH_2), 108.08 (d, $^2J_{C–F} = 22.0$ Hz, C-5), 107.94 (C-3), 120.30 (d, $^3J_{C–F} = 2.60$ Hz, C-13a), 122.60 (d, $^3J_{C–F} = 7.50$ Hz, C-4a), 123.58 (C-10), 123.80 (C-13b), 128.29 (C-8). 132.08 (C-9), 133.87 (C-11), 134.53 (C-11a), 140.92 (d, $^2J_{C–F} = 16.50$ Hz, C-6a), 147.56 (C-7a), 152.17 (C-2), 151.82 (d, $^1J_{C–F} = 246$ Hz, C-6), 166.14 (C(3)$COOH$), 168.17 (C-12), 176.66 (C-4). HRMS (ESI, −ve): m/z calculated for C$_{19}$H$_{13}$FN$_3$O$_4$ [M−H]$^-$: 366.08901, Found: 366.08956. Anal. calcd. for C$_{19}$H$_{14}$FN$_3$O$_4$ (367.33): C, 62.12; H, 3.84; N, 11.44. Found: C, 62.34, H, 3.50; N, 11.52.

Preparation of the test compounds and orlistat for the in vitro PL activity assay

Orlistat (10 mg, Sigma, St. Luis, MO, USA) was dissolved in DMSO (10 mL) to give a stock solution (1 mg/mL), which was used to make six different working solutions with concentrations in the range of 0.625–20 μg/mL. Thereafter, 20 μL aliquots of each working solution were used in the reaction mixture to give final concentrations in the range of 0.0125–0.4 μg/mL. Furthermore, five different working solutions of ciprofloxacin (Dar Al-Dawa, Jordan) in DMSO were prepared with concentrations in the range of 97.5–1,562.5 μg/mL. Thereafter, 20 μL aliquots of each stock solution were used in the reaction mixture to give a final concentration in the range of 1.95–31.25 μg/mL. The test compounds (**11**–**13**) were initially dissolved in DMSO to give three stock solutions, which were subsequently diluted to give five different stock solutions (compounds **11** and **12**: 0.3125–5.0 mg/mL and **13**: 0.15625–2.5 mg/mL). Thereafter, 20 μL aliquots of each stock solution were used in the reaction mixture to give the following final concentration ranges: compounds **11** and **12**: 6.25–100 μg/mL and **13**: 3.125–50 μg/mL.

Quantification of PL activity by spectrophotometric assay

Crude porcine PL type II (0.5 mg/mL, Sigma, St. Luis, MO, USA, EC 3.1.1.3) was suspended in Tris-HCl buffer (2.5 mM, pH 7.4) to a final concentration of 200 units/mL. A 100-μM solution of *para*-nitrophenyl butyrate (*p*-NPB) in DMSO was used as the PL substrate. Aliquots (0.1 mL) of the PL solution were added to the reaction mixtures, and the volumes were made up to 1.0 mL with Tris-HCl buffer. The PL was preincubated with different concentrations of the test material for at least 1 min prior to the addition of the substrate. The reactions were maintained at 37 °C and initiated by the addition of 5 μL of the *p*-NPB substrate solution. The *p*-nitrophenol released during the reaction was measured at 410 nm using a SpectroScan 80D UV–Vis spectrophotometer over a minimum of five time points (1–5 min), against a blank of the same mixture containing

the denatured enzyme. The catalytic activity of PL was determined colorimetrically by measuring its activity toward the hydrolysis of p-NPB to p-nitrophenol. The activity of PL in this reaction was quantified by measuring the increase in the rate of the release of p-nitrophenol from the slope of the linear segment of the absorbance versus time profiles (Bustanji *et al.*, 2011).

The percentage of residual PL activity was determined for all of the test compounds relative to the control compounds, to calculate the concentration required to inhibit the activity of PL by 50 % (i.e., the IC_{50}). All of the assays were performed in triplicate and the calculated activities reported as the mean values $\pm$ SEM ($n = 3$). The PL inhibition values (%) were calculated according to the following formula: Inhibition (%) = $100 - [(B/A) \times 100]$, where A is the PL activity in the absence of an inhibitor or test compound and B is the PL activity in the presence of an inhibitor or test compound.

Molecular modeling

Software and hardware: The following software packages were used in the current study: (1) MarvinSketch (2013), (2) OMEGA (2008), (3) FRED (2009), and (4) Discovery Studio Visualizer (2008).

Docking experiments

The chemical structures of the quinolone derivatives (FQs, **11**, **12**, **13,** and ciprofloxacin) were sketched in MarvinSketch (5.12.3) and saved in the MDL molfile format. A variety of energetically accessible conformers were then generated using the OMEGA software. The OMEGA software generates conformers via a two-stage process that involves the building of the models followed by a torsion search. During the model building stage, an initial 3D structure is assembled from a library of fragments, and the conformations of the fragments are retrieved from pre-generated libraries built within the software. During the torsion search stage, the software generates additional models using particular rule-based torsion angles that are dependent on the molecular environment between the connecting fragments. The resulting conformers are then saved in SD format. The 3D coordinates of PL were obtained from the Protein Data Bank (PDB code: 1LPB, resolution of 2.46 Å) (Egloff *et al.*, 1995). Hydrogen atoms were added to the protein using the Discovery Studio Visualizer templates for protein residues. The docking study was conducted in the presence of explicit water molecules. No energy minimization steps were taken following the addition of the hydrogen atoms. The FQs were docked into the binding

pocket of PL using the FRED software, which takes a target protein structure, a pre-generated multi-conformer database of ligands, a box defining the active site of the protein, and several optional parameters as its input parameters. The protein structure and ligand conformers are treated as rigid entities during the docking simulation process. The docking strategy used by the FRED software exhaustively scores all of the possible poses of each ligand in the active site. All of the different quinolone conformers generated using the OMEGA software were inputted into the FRED software, and the docking settings that succeeded in reproducing the experimental pose of the co-crystallized ligand (CllP, Fig. 3a) (Egloff *et al.*, 1995) were employed. Further details of the FRED parameters used in the current docking simulations have been reported by Bustanji *et al.* (2011).
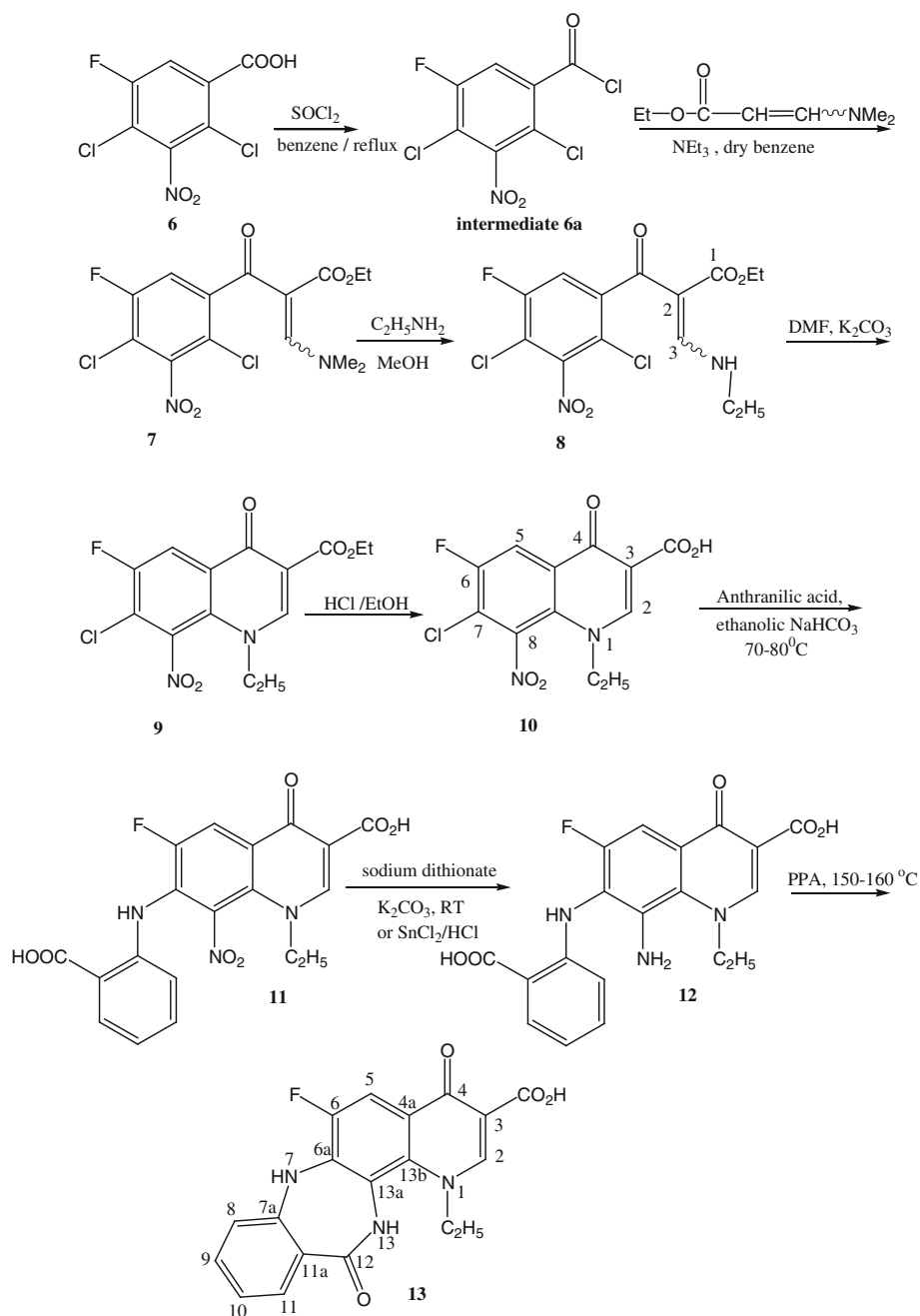
Results and discussion

Synthesis of novel compounds

7-Chloro-1-ethyl-6-fluoro-1,4-dihydro-8-nitro-4-oxoquinoline-3-carboxylic acid (**10**) was prepared from compound **7** according to our previously reported methods, with some minor modifications (Al-Hiari *et al.*, 2007, 2008, 2011). Compound **7** was reacted with ethylamine to give compound **8**, which was subsequently cyclized by treatment with potassium carbonate in DMF (Scheme 1). The resulting ester **9** was hydrolyzed in ethanolic HCl to give the corresponding acid **10**. Compound **11** was synthesized by the reaction of anthranilic acid with compound **10**. The 8-nitro derivative **11** was reduced to the corresponding aniline **12** with aqueous sodium dithionite. This compound could also be reduced with stannous chloride ($SnCl_2$) in aqueous HCl, but this reaction gave a lower yield of the aniline product. Compound **12** was cyclized to quino-benzodiazepine **13** using PPA. Intermediates **7–12** and compound **13** were identified and characterized by IR, MS, and ^1H, and ^{13}C NMR spectroscopic analyses. The different signal for the protons and carbons was assigned using DEPT and 2D (COSY, HMQC, and HMBC) experiments.

The ^1H NMR spectra of all of the synthesized compounds contained a doublet for H-5 ($J_{H-F} = 11–13$ Hz) at ~ 8.0 ppm. The splitting of this signal was caused by the vicinal fluorine and indicated the presence of an FQ nucleus in all of these compounds. Similarly, the singlet for H-2 at ~ 9.0 ppm effectively confirmed that synthon **10** had been formed successfully. Similar patterns were also observed for compounds **11–13**. The ^1H NMR spectra of compounds **11** and **12** contained two new broad singlets in the ranges of 9.35–10.32 and 13.65–15.20 ppm, which

Scheme 1 Synthetic pathway of novel compounds **7–13**

were assigned to the NH–Ar and Ar–COOH protons, respectively. These signals effectively confirmed that the aminobenzoic acid side chain had been effectively incorporated into compounds **11** and **12**. Furthermore, the appearance of a broad singlet at 5.74 ppm that integrated for two protons indicated that the reduction step had proceeded successfully to give compound **12**. The appearance of a singlet at ∼10.0 ppm that was assigned to the amide N(13)–H confirmed that **12** had undergone the cyclization reaction to give compound **13**.

All of the carbons belonging to the skeleton of the fused benzenoid ring were recognizable by the splitting patterns resulting from their interaction with the fluorine atom and their long-range coupling to the surrounding protons. The ^{13}C NMR spectra of compounds **10–13** contained a doublet ($^{1}J_{C-F} = 250$ Hz) at ∼150 ppm for C-6, which indicated the presence of the FQ nucleus in all of these compounds. The splitting of the neighboring carbon signals at C-5, C6a, and C-7 into doublet peaks in these compounds ($^{2}J_{C-F}$ ∼20 Hz) effectively confirmed that they were all vicinal to

Table 1 Pancreatic lipase IC$_{50}$ values for the investigated concentrations of test compounds and orlistat. Results are mean ± SEM ($n = 3$ independent replicates)

Test Compound	IC$_{50}$ (µg/mL)	IC$_{50}$ (µM)	ClogP*
11	7.60 ± 0.70	18.4 ± 1.6	4.65
12	10.30 ± 0.70	26.7 ± 1.7	3.35
13	10.70 ± 1.40	29.1 ± 1.4	2.79
Ciprofloxacin	23.60 ± 1.50	71.1 ± 4.7	−1.15
Orlistat	0.11 ± 0.01	0.23 ± 0.01	8.61

* ClogP value was calculated using ChemDraw Ultra (V.8, 2003)

a fluorine atom. The appearance of signals at 165.0 ppm (–COOH) and 175.0 ppm (C=O) in the ^{13}C NMR spectrum of compound **10** confirmed its structure. The presence of an extra carbon peak (singlet) in the range of 165.0–172.0 ppm confirmed the introduction of the aminobenzoic acid side chain in **11**.

FQs in vitro inhibition of PL activity

The balance of energy storage is regulated by lipases in the intestine and adipose tissues, and lipases consequently represent important drug discovery targets because they play a central role in metabolism. Many lipase inhibitors have been isolated from natural sources, as well as being derived from the synthesis of substrate analogs or biomimetic materials. Several synthetic inhibitors of pancreatic triacylglycerol lipase have been developed and optimized for use in conjunction with inhibitors of other lipase targets for the dual management of obesity and diabetes (Padwal, 2008; Wierzbicki et al., 2012). The aim of the current study is to develop new potential PL inhibitors containing FQs. The anti-lipase activities of compounds **11–13** are shown in Table 1 and in Fig. 2. These compounds showed dose-dependent anti-PL activity. The IC$_{50}$ values of compounds **11–13** were 18.4, 26.7, and 29.1 µM, respectively. In contrast, ciprofloxacin gave an IC$_{50}$ value of 71.1 µM. The IC$_{50}$ of the standard compound orlistat was 0.2 µM, which was comparable to the values cited in the literature (Habtemariam, 2012; Mohammad et al., 2013).
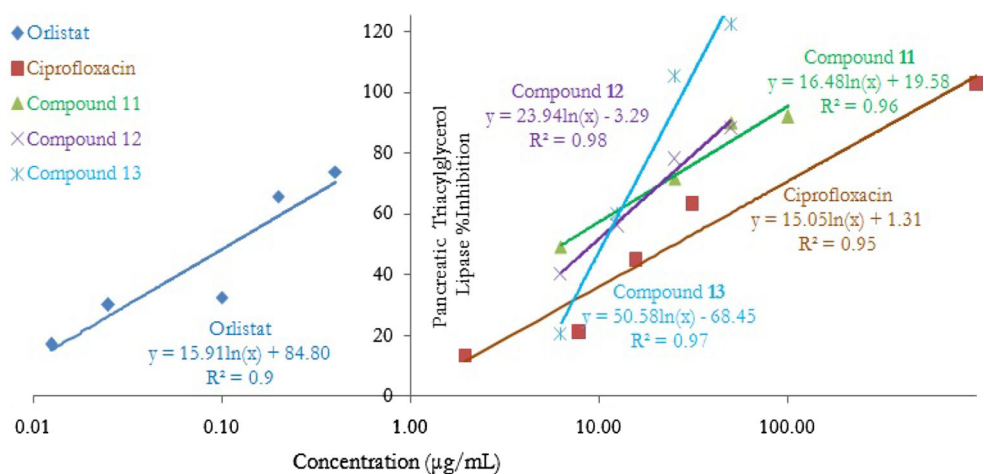
Compounds **11–13** exhibited significant in vitro inhibitory activity toward PL. It is possible that the activities of compounds **11–13** could be related to their lipophilicity. Compound **11**, for example, showed the highest inhibitory activity of these compounds (IC$_{50}$ = 18.4 µM) as well as the highest ClogP value of 4.65 (Table 1). In contrast, compounds **12** and **13** showed lower PL inhibitory activities with ClogP values of 3.35 and 2.79, respectively. The low activity of ciprofloxacin could be attributed to its low ClogP value (Table 1). It is well known that the lipophilic catalytic site of the enzyme is perfectly suited to the

lipophilic nature of orlistat (ClogP 8.61) (Bentley et al., 2012). These results, therefore, indicate that there is a linear trend between the lipophilicity of the inhibitors and their inhibitory activity (King et al., 2009).
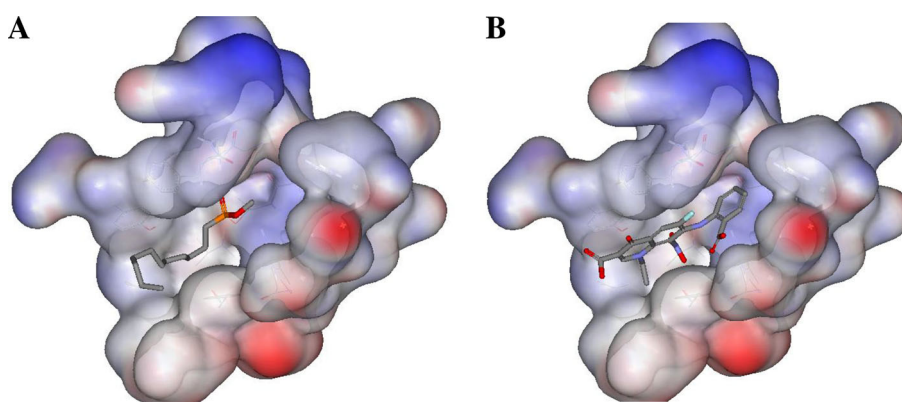
Molecular modeling and docking

Scaffold similarities in the structures of reported iso-quinoline- and quinolone-based PL inhibitors attracted our attention to investigate the inhibitory activities of the synthetic FQs **11–13** toward PL. Our selection was based entirely on the simple postulation that similar chemical structures could have similar biological activities (Polur et al., 2011). To begin, we evaluated the possibility of FQ–PL binding via molecular docking simulations, and the FQs were docked into the binding pocket of PL (PDB code: 1LPB). The docking process consists of two stages, including (i) predicting the pose (conformation and orientation) of the ligand into the binding cleft, and (ii) estimating the biological activity through an evaluation of the interactions between the compounds and their potential targets (scoring). The final docked poses were selected according to their scores. The docking study was carried out using the FRED docking engine (FRED 2009). Simulated molecular docking, however, requires the user to provide FRED with an optimal set of parameters for the docking experiment. In the current study, we used the parameters that had been validated in silico by the self-docking of the co-crystallized ligand. These parameters were further validated experimentally when they were used to successfully predict the bioactivity of some natural PL inhibitors (Bustanji et al., 2011; Mohammad et al., 2013). The FQs were then docked into the binding pocket of PL using these optimal docking parameters, and all four of these compounds were predicted by simulated docking to bind within the active site of PL. Fig. 3 shows the highest ranking pose for the docking of compound **11** within the binding site of PL. Table 2 shows the ranking of the docked FQs according to their estimated binding affinities, which had been calculated using the Chemgauss2 scoring function. The results of our preliminary docking study encouraged us for further investigate the inhibitory activities of the FQs, and all of the docked FQs were subjected to an in vitro activity bioassay. The in vitro activity was expressed as the concentration of FQ required to inhibit the PL activity by 50 % (IC$_{50}$) using p-NPB as a substrate. As suggested by molecular docking simulation, the four FQs did show inhibitory activity toward PL in vitro (Table 2). As shown in Table 2, there was a clear successful ranking correlation between the Chemgauss2 scoring function and the IC$_{50}$ values for the designed compounds. These findings validate the effectiveness of the docking

Fig. 2 In vitro inhibitory activity of test compounds (**11–13**), ciprofloxacin and orlistat on pancreatic lipase. Results per each compound are mean ± SEM (n = 3 independent replicates)

Fig. 3 The solvent accessible surface area of the binding site of pancreatic lipase (PDB code: 1LPB) and **a** the co-crystallized inhibitor (CllP), **b** quinolone derivative (**11**)

conditions in terms of their ability to predict the relative affinities of different compounds and thus the bioactivities of the docked compounds.

On the molecular level, several significant binding interactions can be observed between the docked structures and the PL, as shown in Fig. 3. A comparison of the docked pose of the most potent FQ (**11**, Fig. 4a) with the co-crystallized ligand within the binding site of PL highlights the similarities in their binding profiles. The quinolone ring of **11** potentially undergoes hydrophobic interactions with several key amino acid residues, including Phe-77, Ile-209, Pro180, Tyr-114, and Phe-215, which collectively form a lipophilic pocket within the binding pocket of the PL. Furthermore, the carboxylate group of **11** lies within the positive electrostatic attractive field of the basic amino acid residues Arg-256, His-263, and His-151. The most potent FQ (**11**, IC_{50} = 18.4 μM) also forms a strong hydrogen bond with Ser-152 (within 2.4 Å, Fig. 4a), which stabilizes the ligand–protein complex and contributes to the relatively high affinity of **11** for the protein. Similarly, the co-crystallized ligand has analogous interactions where the hydrophobic aliphatic chain of the co-crystallized ligand extends into the lipophilic site to form a
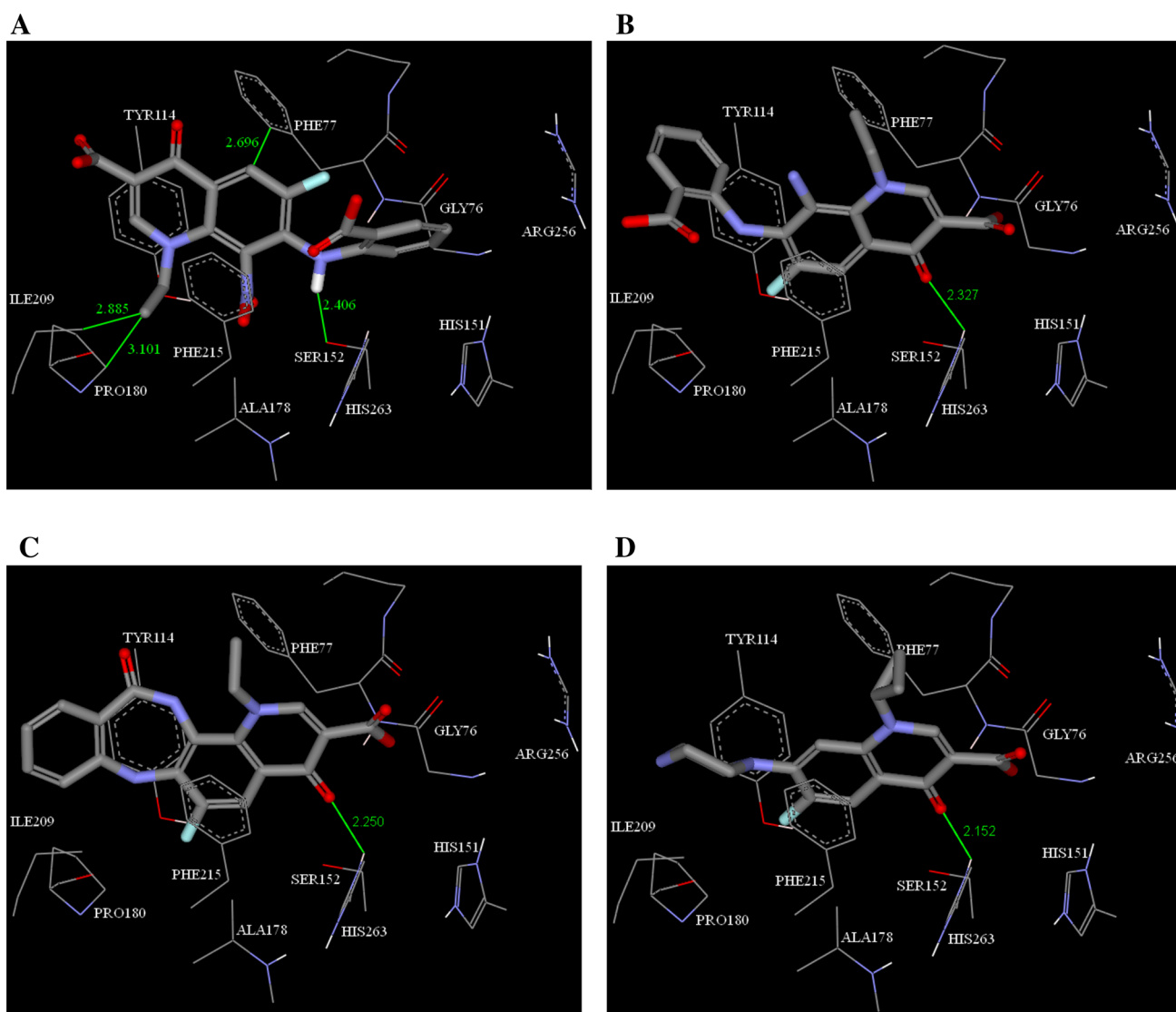
Table 2 The docked quinolone derivatives with their IC_{50} values ranked according to their estimated binding affinity

Rank	TTLs	Chemgauss2 score	IC_{50}(μg/mL)
1	**11**	63.93	7.60 ± 0.7
2	**12**	58.83	10.3 ± 0.7
3	**13**	56.10	10.7 ± 1.4
4	Ciprofloxacin	52.19	23.6 ± 1.5
	Orlistat[a]	–	0.114 ± 0.0

Rank rank according to the estimated binding affinity calculated using FRED Chemgauss2 scoring function

[a] Orlistat is used as a positive control

network of hydrogen bonds with Ser-152, His-263, Leu-135, and Phe-77 (Bustanji *et al.*, 2011). Within the active site of PL, the His-263, Asp-176, and Ser-152 residues form the catalytic triad of the lipolytic site. Furthermore, chemical modification of the Ser-152 residue has been shown to have an adverse effect on the enzymatic activity of PL, indicating that this residue is critical to the catalytic activity (Winkler *et al.* 1990). It is, therefore, not surprising that the compounds bind strongly to the catalytic triad, especially Ser-152, to inhibit the lipolytic activity. While

Fig. 4 Detailed view of the docked pose of quinolone derivatives and the corresponding interacting amino acids within the binding site of pancreatic lipase enzyme (PDB code: 1LPB, **a** 11, **b** 12, **c** 13, **d** ciprofloxacin)

the remaining three FQs (**12**, **13,** and ciprofloxacin) could undergo similar binding interactions (Fig. 4b, c, d), they lack the Ser152-hydrogen bond attachment and would, therefore, have lower potential hydrophobic interactions with Phe-77 and Ile-209, as shown by FQ **11** (Fig. 4a).

Conclusions

Unprecedentedly, this work revealed novel FQs as PL inhibitors. Three newly synthesized FQs (**11**, **12**, and **13**) were tested with respect to their in vitro anti-lipase efficacy and potency properties, and gave IC_{50} values in the range of 18.4–29.1 μM against PL whereas the standard drug orlistat

gave an IC_{50} of 0.2 μM. These data were supported by docking studies, which suggested that the FQs synthesized in the current study could be acting via a similar mechanism to that of orlistat. Subsequent lead optimization and structural modification studies would be required to improve the anti-lipase activity, potency, and selectivity of this novel series of FQs and to lessen their anti-bacterial activity. Downstream studies of the in vivo tolerance, efficacy, and safety of these compounds may also be required in the future.

References

Al-Hiari YM, Al-Mazari IS, Shakya AK, Darwish RM, Abu-Dahab R (2007) Synthesis and antibacterial properties of new 8-nitro fluoroquinolone derivatives. Molecules 12(6):1240–1258

Al-Hiari YM, Abu-Dahab R, El-Abadelah MM (2008) Heterocycles [*h*]-fused onto 4-oxoquinoline-3-carboxylic acid, part VIII. Convenient synthesis and antimicrobial properties of substituted hexahydro[1,4]diazepino[2,3-*h*]quinoline-9-carboxylic acid and its tetrahydroquino[7,8-*b*]benzodiazepine analog. Molecules 13(11):2880–2893

Al-Hiari YM, Shakya AK, Alzweiri MH, Al-Qarim TM, Shattat GF, El-Abadelah MM (2011) Synthesis and antibacterial properties of new *N4*-acetylated hexahydro-2,7-dioxopyrido[2,3*f*]quinoxaline-8-carboxylic acids. J Enzyme Inhib Med Chem 26(5):649–656

Baretic M (2012) Targets for medical therapy in obesity. Dig Dis 30(2):168–172

Bentley D, Young AM, Rowell L, Gross G, Tardio J, Carlile D (2012) Evidence of a drug–drug interaction linked to inhibition of ester hydrolysis by orlistat. J Cardiovasc Pharmacol 60(4):390–396

Bustanji Y, Al-Masri IM, Mohammad M, Hudaib M, Tawaha K, Tarazi H, Alkhatib HS (2011) Pancreatic lipase inhibition activity of trilactoneterpenes of *Ginkgo biloba*. J Enzyme Inhib Med Chem 26(4):453–459

Charmot D (2012) Non-systemic drugs: a critical review. Curr Pharm Des 18(10):1434–1445

Chen KY, Chang SS, Chen CY (2012) In silico identification of potent pancreatic triacylglycerol lipase inhibitors from traditional Chinese medicine. PLoS One 7(9):e43932

Clifton JD, Lucumi E, Myers MC, Napper A, Hama K, Farber SA, Smith AB 3rd, Huryn DM, Diamond SL, Pack M (2010) Identification of novel inhibitors of dietary lipid absorption using zebrafish. PLoS One 5(8):e12386

De la Cruz A, Elguero J, Gotor V, Goya P, Martinez A, Moris F (1991) Lipase-mediated acylation of acyclonucleosides: application to novel fluoroquinolone derivatives. Synth Commun 21(14):1477–1480

Discovery Studio Visualizer (2008) Version 2.0.1.7347, Accelrys Software Inc., San Diego. www.accelrys.com. Accessed 1 May 2013

Ebdrup S, Sørensen LG, Olsen OH, Jacobsen P (2004) Synthesis and structure–activity relationship for a novel class of potent and selective carbamoyl-triazole compound based Inhibitors of hormone sensitive lipase. J Med Chem 47(2):400–410

Egloff MP, Marguet F, Buono G, Verger R, Cambillau C, Van-Tilbeurgh H (1995) The 2.46 Å resolution structure of the pancreatic lipase-colipase complex inhibited by a C11 alkyl phosphonate. Biochemistry 34(9):2751–2762

FRED (2009) Version 2.2.5, OpenEye scientific software Inc., Santa Fe, NM. http://www.eyesopen.com. Accessed 1 May 2013

Habtemariam S (2012) The anti-obesity potential of sigmoidin A. Pharm Biol 50(12):1519–1522

King AR, Lodola A, Carmi C, Fu J, Mor M, Piomelli D (2009) A critical cysteine residue in monoacylglycerol lipase is targeted by a new class of isothiazolinone-based enzyme inhibitors. Br J Pharmacol 157(6):974–983

MarvinSketch (2013) Version 5.12.3, ChemAxon. http://www. ChemAxon.com. Accessed 1 May 2013

Mohammad M, Al-masri IM, Issa A, Khdair A, Bustanji Y (2013) Inhibition of pancreatic lipase by berberine and dihydroberberine: an investigation by docking simulation and experimental validation. Med Chem Res 22(5):2273–2278

Ninomiya K, Matsuda H, Shimoda H, Nishida N, Kasajima N, Yoshino T, Morikawa T, Yoshikawa M (2004) Carnosic acid, a new class of lipid absorption inhibitor from sage. Bioorg Med Chem Lett 14(8):1943–1946

OMEGA (2008) Version 2.3.2, OpenEye scientific software Inc., Santa Fe, NM. http://www.eyesopen.com. Accessed 1 May 2013

Padwal R (2008) Cetilistat, a new lipase inhibitor for the treatment of obesity. Curr Opin Investig Drugs 9(4):414–421

Polur H, Joshi T, Workman CT, Lavekar G, Kouskoumvekaki I (2011) Back to the roots: prediction of biologically active natural products from Ayurveda traditional medicine. Mol Inform 30(2–3):181–187

WHO (2012) Obesity and overweight. http://www.who.int/mediacentre/factsheets/fs311/en/. Accessed 15 Sep 2012

Wierzbicki AS, Hardman TC, Viljoen A (2012) New lipid-lowering drugs: an update. Int J Clin Pract 66(3):270–280

Winkler FK, D'Arcy A, Hunziker W (1990) Structure of human pancreatic lipase. Nature 343(6260):771–774

Witter D, Castelhano A (2006) Pancreatic lipase inhibitor compounds, their synthesis and use. US Patent 7,064,122 B2, Jun 2006

Yamada Y, Kato T, Ogino H, Ashina S, Kato K (2008) Cetilistat (ATL-962), a novel pancreatic lipase inhibitor, ameliorates body weight gain and improves lipid profiles in rats. Horm Metab Res 40(8):539–543